


Article

Trimethylamine N-Oxide (TMAO) and Trimethylamine (TMA) Determinations of Two Hadal Amphipods

Qi Liu ^{1,2}, Shouwen Jiang ³, Wenhao Li ³, Binbin Pan ¹ and Qianghua Xu ^{1,2,4,*} 

¹ Shanghai Engineering Research Center of Hadal Science & Technology, College of Marine Sciences, Shanghai Ocean University, Shanghai 201306, China; m190200531@st.shou.edu.cn (Q.L.); bbpan@shou.edu.cn (B.P.)

² Key Laboratory of Sustainable Exploitation of Oceanic Fisheries Resources, Ministry of Education, College of Marine Sciences, Shanghai Ocean University, 999 Huchenghuan Road, Lingang New City, Shanghai 201306, China

³ Key Laboratory of Aquaculture Resources and Utilization, Ministry of Education, College of Fisheries and Life Sciences, Shanghai Ocean University, Shanghai 201306, China; swjiang@shou.edu.cn (S.J.); wh-li@shou.edu.cn (W.L.)

⁴ National Distant-Water Fisheries Engineering Research Center, Shanghai Ocean University, Shanghai 201306, China

* Correspondence: qhxu@shou.edu.cn

Abstract: Hadal trenches are a unique habitat with high hydrostatic pressure, low temperature and scarce food supplies. Amphipods are the dominant scavenging metazoan species in this ecosystem. Trimethylamine (TMA) and trimethylamine oxide (TMAO) have been shown to play important roles in regulating osmotic pressure in mammals, hadal dwellers and even microbes. However, the distributions of TMAO and TMA concentrations of hadal animals among different tissues have not been reported so far. Here, the TMAO and TMA contents of eight tissues of two hadal amphipods, *Hirondellea gigas* and *Alicella gigantea* from the Mariana Trench and the New Britain Trench, were detected by using the ultrahigh performance liquid chromatography–mass spectrometry (UPLC-MS/MS) method. Compared with the shallow water Decapoda, *Penaeus vannamei*, the hadal amphipods possessed significantly higher TMAO concentrations and a similar level of TMA in all the detected tissues. A higher level of TMAO was detected in the external organs (such as the eye and exoskeleton) for both of the two hadal amphipods, which indicated that the TMAO concentration was not evenly distributed, although the same hydrostatic pressure existed in the outer and internal organs. Moreover, a strong positive correlation was found between the concentrations of TMAO and TMA in the two hadal amphipods. In addition, evolutionary analysis regarding FMO3, the enzyme to convert TMA into TMAO, was also conducted. Three positive selected sites in the conserved region and two specific mutation sites in two conserved motifs were found in the *A. gigantea* FMO3 gene. Combined together, this study supports the important role of TMAO for the environmental adaptability of hadal amphipods and speculates on the molecular evolution and protein structure of FMO3 in hadal species.

Keywords: hadal; amphipod; TMAO; FMO3; molecular evolution



Citation: Liu, Q.; Jiang, S.; Li, W.; Pan, B.; Xu, Q. Trimethylamine N-Oxide (TMAO) and Trimethylamine (TMA) Determinations of Two Hadal Amphipods. *J. Mar. Sci. Eng.* **2022**, *10*, 454. <https://doi.org/10.3390/jmse10040454>

Academic Editor: Taewon Kim

Received: 13 February 2022

Accepted: 18 March 2022

Published: 23 March 2022

Publisher's Note: MDPI stays neutral with regard to jurisdictional claims in published maps and institutional affiliations.



Copyright: © 2022 by the authors. Licensee MDPI, Basel, Switzerland. This article is an open access article distributed under the terms and conditions of the Creative Commons Attribution (CC BY) license (<https://creativecommons.org/licenses/by/4.0/>).

1. Introduction

The hadal zone is the deepest area of the ocean, extending from 6000 to 11,000 m in depth from the ocean surface and accounts for 45 percent of the total ocean depth range [1]. The hadal region represents 1–2% of the global benthic area, consisting mainly of trenches characterized by high hydrostatic pressure (HHP), low temperature, darkness, and low organic matter [2–6]. As the deepest ecosystem, the hadal zone is one of the most unique ecosystems on earth. Compared with the shallow sea, HHP is a major feature that distinguishes hadal trenches from other ecosystems. HHP is unique in that it manifests as the largest continuous, stable gradient of any stressor in the hadal zone, reaching about 100 Mpa in the deepest area [7,8].

However, despite such harsh conditions, there are still many species living in hadal habitats. According to extensive hadal sampling records, amphipods are the most dominant decomposers in hadal environments, which are widely distributed in many trenches, with habitats up to 10,000 m deep, and are easy to trap [9–11]. Among them, *Alicella gigantea* and *Hirondellea gigas* are reported as the most common amphipods in the hadal environment. *A. gigantea* is the largest known amphipod, reaching 340 mm in length [12,13]; *H. gigas* can even be found and captured at depths of 11,000 m [14]. Therefore, studies regarding hadal amphipods' adaptations can give us insights into the adaptive mechanisms of other species in hadal environments.

Generally, HHP may break protein structure [15], cause DNA breakage and damage [16] and reduce cell membrane fluidity [17]. To survive in the hadal environment, the extrinsic adaptation mechanism and intrinsic adaptation were needed [18]. The extrinsic adaptation includes different molecular and chemical chaperones. The molecular chaperones such as the heat-shock proteins (HSPs) are well known for resisting apoptosis, assisting transmembrane transport, and helping protein folding and transporting [19,20]. For deep-sea species, chemical chaperones, especially the organic osmolytes, have been reported to play important roles in adapting to HHP. These are the most important small molecules found in many organisms to maintain cell volume and protein function when facing stress, mainly including ammonia nitrogen compounds, amino acid derivatives, polyols, sugars and urea [21]. TMA (trimethylamine) is an important ammonia–nitrogen compound which is mainly formed by the consumption of carnitine choline by gut microorganisms [22]. TMAO (trimethylamine oxide) is an important osmotic regulator produced by TMA oxidation under the action of the flavin monooxygenases (FMOs) [23]. TMAO is a powerful protein stabilizer commonly found in marine fish muscle tissue, which can mitigate the effects of hydrostatic pressure on protein stability and restore denatured proteins to their natural structure [24]. TMAO is a universal protein stabilizer and counteractant for resisting urea damage [21]. TMAO can also act as a piezolyte, which could bind with water, prevent water molecules clumping together and avoid the protein aggregations [25,26].

TMAO concentrations are reported to increase gradually with the increase in depth, suggesting its important function for the hadal species [21,27]. In chondrichthyan species (Chondrichthyes), TMAO content increases from ~150 mmol/kg to ~200 mmol/kg with the depth increasing from 500 to 1500 m [28]. In teleost fish, muscle TMAO content ranges from less than 50 mmol/kg in shallow species to nearly 400 mmol/kg when the depth is nearly 8000 m [24]. As for invertebrates (such as squid, decapods and amphipods), TMAO has been found to increase linearly with depth. For example, TMAO content in muscle of the decapod *Pandalus danae* increases linearly from 76 mmol/kg to 299 mmol/kg with the depth increasing from 0 to 2850 m [29]. As for amphipods, TMAO concentrations were reported ranging from less than 15 mmol/kg in shallow sea species to above 80 mmol/kg in a deep-sea sample [30,31]. It should be noticed that, for a decapod at 6000 m depth, the TMAO content in white muscle is about 270 mmol/kg, whereas the TMAO in hemolymph is only 12.9 mmol/kg [32], which indicates the great variations of TMAO concentration between tissues. However, the distributions of TMAO concentrations of hadal species among different tissues have not been reported so far.

Hadal environment intrinsic adaptation mainly refers to the evolutionary adaptation of the amino acid sequence of protein itself, which includes amino acid substitutions in some specific sites and protein structure changes [33,34]. FMOs belong to a subfamily of B monooxygenases and are conserved in all phyla. Their main function is to add molecular oxygen to lipophilic compounds [35,36]. There are five different functional FMO in adult mammals, numbered from one to five, and FMO3 is the most important TMA oxidase expressed in the liver [34,37]. The oxidation activity of FMO is very efficient because it does not require the presence of substrates to initiate the catalytic cycle. The prosthetic group was offered by flavin adenine dinucleotide (FAD), nicotinamide adenine dinucleotide phosphate hydrogen (NADPH) was used as a hydride donor, and oxygen existed as cosubstrate [38]. The FMO expression could help cells to be resistant to multiple stressors, including high-

pressure stress, heavy metal contaminations, free radical generator paraquat, UV radiation and the mitochondrial toxin rotenone [34,37]. However, little is known about the FMO in hadal amphipods.

Therefore, we decided to measure the TMAO and TMA content in two hadal amphipod species, *A. gigantea* and *H. gigas*, and compared them with the content in a shallow-water decapod species, *Penaeus vannamei*. Evolutionary analysis regarding to the hadal amphipods' FMO3 was also conducted. Our research on TMAO and TMA content in different tissues in the hadal amphipods provides new insights into the possible molecular adaptation mechanisms of the hadal amphipods.

2. Materials and Methods

2.1. Source of the Sample

Two hadal amphipod species, *Hirondellea gigas* and *Alicella gigantea*, were collected from the Mariana Trench (10,839 m, 11.38° N 142.42° E) and the New Britain Trench (8824 m, 7.02° S 149.16° E) in the west Pacific Ocean. Amphipod samples were collected by the autonomous deep-ocean lander vehicle launched from the “Zhang Jian” research vessel over the course of four sampling campaigns [38]. The detailed information about the lander vehicle and sampling were described in our previous study [38]. Once collected on-board, each amphipod sample was placed in a separate zip-lock bag and was immediately frozen upon recovery at -80°C . One shallow-water decapod species, *P. vannamei*, collected from Qingdao coastal area with the depth ranging from 50~75 m, was also used in this study.

2.2. Pretreatment of Experimental Samples

Hirondella gigas, *Alicella gigantea* and *Penaeus vannamei* were dissected and eight tissues (eye, brain, exoskeleton, gonad, fat, gut, muscle and liver) were obtained for the following experiment. Each tissue was extracted from 10~30 individuals and the measurements for each tissue were repeated 9 times.

Twenty milligrams of samples from each tissue were stored in a centrifugal tube, and 1200 μL solution (CH_3OH : water = 4:1) was added. Then, vibration crushing was performed on a high-throughput tissue crusher to crush the tissue samples. Ice bath ultrasonic extractions were subsequently conducted three times. The tissue suspensions were stored in the refrigerator at -20°C for 20 min and centrifuged for 10 min at 13,000 rpm at 4°C . The supernatant was collected and diluted 20 times. Four hundred microliters of diluted liquid were sucked out and then incorporated into the sample by chromatography using the LC-MS and stored in a 4°C refrigerator for further LC-MS, UPLC tests and analysis.

2.3. Settings of the UPLC-MS/MS Parameters

The quantifications of TMAO and TMA were performed by UPLC-MS/MS (WATERS Inc., Milford, MA, USA). The chromatographic separation was carried out on an Infinity II HILIC column. The flow rate was maintained at 0.2 mL/min, and the column was heated to 30°C . The instrument parameters for WATERS UPLC-MS/MS analysis are as follows: nitrogen drying gas temperature 300°C , nitrogen sheath gas temperature 250°C , nitrogen drying gas flow 5 L min^{-1} , nitrogen sheath gas flow 11 L min^{-1} , capillary voltage 3500 V, nebulizer pressure 45 psi and nozzle voltage 500 V. The information regarding untested compounds and internal standards was detected by characteristic precursor-product ion transitions.

The detection was carried out by using a triple quadrupole mass spectrometer in the positive ion mode in the multiple reaction monitoring (MRM) modes. The sample concentrations were determined from calibration curves using a peak area ratio of the analyte to its isotope [39].

2.4. Evolutionary Analysis and Protein Crystal Structure Prediction of FMO3

The BLAST program of National Center for Biotechnology Information (NCBI) was used to search deduced amino acid sequences of FMO3 derived from selected crustacean.

ClustalW in MEGA X was used for multiple sequence alignment. Phylogenetic tree was constructed by ML method with the bootstrap of 1000 and Figtree was used for beautification. PFAM, Interpro and SMART databases were used to annotate the deduced FMO3 of *A. gigantea* and *P. vannamei* for structural domain analysis. Conserved motif sequences were predicted from PFAM database. Evolutionary analysis was conducted through the Branch site model in Preset Mode in EasyCodeml (Version 1.4) [40]. Through the likelihood ratio test (LRT) test, the crystal structure model of FMO3 and FAD ligand was carried out by the I-TASSER database.

3. Results

3.1. TMAO and TMA Concentrations of the Two Hadal Amphipods

In this study, two compounds (TMAO and TMA) in eight tissues (eye, brain, muscle, exoskeleton, gonad, fat, gut, muscle and liver) of two hadal amphipod species (*A. gigantea* and *H. gigas*) and one shallow-water decapod, *P. vannamei*, were determined. All the TMAO and TMA concentrations are shown in Tables 1 and 2, respectively. It was shown that the order of TMAO mean content level is *A. gigantea* > *H. gigas* > *P. vannamei* (Figure 1). The two hadal amphipods (*A. gigantea* and *H. gigas*) have a higher level of TMAO, even up to 10 times higher than that of their shallow-water counterpart (*P. vannamei*) (Figure 1a). However, the order of TMA mean level of the species is *P. vannamei* > *H. gigas* > *A. gigantea*, which was quite different from the TMAO (Figure 1b).

Table 1. The trimethylamine oxide (TMAO) content (unit: mmol/kg wet weight; mean \pm SD) across eight tissues in three species.

Tissue	Tissue Trimethylamine Oxide (TMAO) Content (mmol/kg)			Significant Difference		
	<i>A. gigantea</i>	<i>H. gigas</i>	<i>P. vannamei</i>	Ag-Hg	Ag-Pv	Hg-Pv
eye	68.52 \pm 12.36	42.80 \pm 2.26	2.49 \pm 0.44	***	***	***
brain	66.69 \pm 14.87	18.99 \pm 7.93	1.96 \pm 0.75	***	***	**
exoskeleton	55.47 \pm 11.76	31.62 \pm 9.56	2.75 \pm 0.80	***	***	***
gonad	43.87 \pm 1.16	15.70 \pm 5.81	1.82 \pm 0.28	***	***	***
fat	40.55 \pm 7.12	22.22 \pm 5.13	2.88 \pm 0.13	***	***	***
gut	34.53 \pm 19.78	28.12 \pm 8.38	2.22 \pm 0.32	-	***	***
muscle	27.36 \pm 16.02	23.09 \pm 21.13	2.48 \pm 0.65	-	**	*
liver	20.48 \pm 12.20	16.24 \pm 6.44	2.84 \pm 0.32	**	****	**

* represents significant difference ($p < 0.05$), ** represents significant difference ($p < 0.01$), and *** represents significant difference ($p < 0.001$).

Table 2. The trimethylamine (TMA) content (unit: mmol/kg wet weight; mean \pm SD) across eight tissues in three species.

Tissue	Tissue Trimethylamine (TMA) Content (mmol/kg)			Significant Difference		
	<i>A. gigantea</i>	<i>H. gigas</i>	<i>P. vannamei</i>	Ag-Hg	Ag-Pv	Hg-Pv
eye	5.48 \pm 3.68	7.99 \pm 0.40	7.89 \pm 1.55	-	-	-
brain	4.02 \pm 1.60	3.40 \pm 0.85	6.52 \pm 0.99	-	***	***
exoskeleton	6.67 \pm 3.90	4.90 \pm 2.51	4.97 \pm 2.09	-	-	-
gonad	5.65 \pm 4.52	2.98 \pm 0.66	7.77 \pm 2.98	-	-	**
fat	3.13 \pm 0.93	3.08 \pm 0.91	3.67 \pm 2.50	-	-	-
gut	3.55 \pm 2.37	3.98 \pm 1.35	12.93 \pm 5.26	-	***	***
muscle	2.09 \pm 1.11	7.12 \pm 12.41	3.65 \pm 0.96	-	**	**
liver	3.08 \pm 1.13	3.07 \pm 0.82	7.08 \pm 1.82	-	***	***

** represents significant difference ($p < 0.01$), and *** represents significant difference ($p < 0.001$).

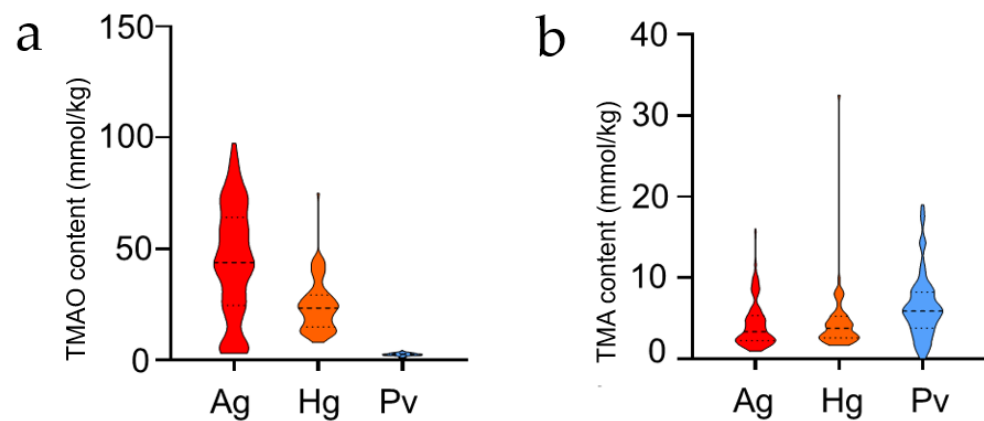


Figure 1. (a,b) Violin diagram of total TMAO and TMA content of two hadal amphipods and a shallow water decapods *P. vannamei*. Red represents *A. gigantea*, orange represents *H. gigas*, and blue represents *P. vannamei*.

Except the comparison with *P. vannamei*, we also compared our study with the reported TMAO concentrations in amphipod species [30,41]. The comparisons are shown in Table 3. Generally, TMAO concentrations in the hadal *A. gigantea* and *H. gigas* are higher than those of the shallow amphipod in Lake Baikal (Table 3). Meanwhile, it can be easily concluded that the TMAO concentration increases generally with increasing depth. As for hadal *H. gigas*, the TMAO concentration of the combined tissues (our study) is closed to the data of the whole body in Downing's study [30].

Table 3. The TMAO concentrations of amphipods from fresh water and marine environments (unit: mmol/kg wet weight).

Species	Tissue	Depth	Location	TMAO	Reference
<i>Megalorchestia columbiana</i>	whole body	−1 m	Sandy beach	15	Downing et al., 2018
<i>Anisogammarus pugettensi</i>	whole body	0.1 m	Sandy beach	12	Downing et al., 2018
<i>Acanthogammarus lappadeus</i>	muscle	50 m	Lake Baikal	6.0	Zerbst et al., 2005
<i>Acanthogammarus grewingki</i>	muscle	170–930 m	Lake Baikal	18.1–28.4	Zerbst et al., 2005
<i>Acanthogammarus albus</i>	muscle	200 m	Lake Baikal	16.1	Zerbst et al., 2005
<i>Scypholanceola aestiva</i>	whole body	763 m	Tidepool	17	Downing et al., 2018
<i>Acanthogammarus reicherti</i>	muscle	930 m	Lake Baikal	31.6	Zerbst et al., 2005
<i>Ceratogammarus dybowskii</i>	muscle	930–1170 m	Lake Baikal	43.3–47.3	Zerbst et al., 2005
<i>Parapallasea lagowskii</i>	muscle	1170 m	Lake Baikal	32.0	Zerbst et al., 2005
<i>Valettietta sp.</i>	whole body	1561 m	Southwest of Oahu	30	Downing et al., 2018
<i>Paralicella tenupies</i>	whole body	3569–4779 m	Kermadec Trench	45–50	Downing et al., 2018
<i>Eurythenes gryllus</i>	whole body	3865–4817 m	Kermadec Trench	26–42	Downing et al., 2018
<i>Cyclocaris</i>	whole body	4897 m	Marina Trench	25	Downing et al., 2018
<i>Bathycallisoma schellenbergi</i>	whole body	5958–9198 m	Kermadec Trench	46–82	Downing et al., 2018
<i>Abyssorchomene musculosus</i>	whole body	6081 m	Marina Trench	30	Downing et al., 2018
<i>Hirondellea gigas</i>	whole body	6974–10,991 m	Marina Trench	38–64	Downing et al., 2018
<i>Hirondellea dubia</i>	whole body	7515–10,005 m	Kermadec Trench	56–75	Downing et al., 2018
<i>Princaxelia jamiesoni</i>	whole body	8189 m	Marina Trench	43	Downing et al., 2018
<i>Alicella gigantea</i>	combined	8824 m	New Britain Trench	20–68	This study
<i>Hirondellea gigas</i>	combined	10,839 m	Marina Trench	15.7–42.8	This study

Note: Downing et al., 2018 [32]; Zerbst et al., 2005 [41].

The mean TMAO and TMA content (mmol/kg) and standard deviations of eight tissues in three species are shown in Figure 2. It was clearly shown that the hadal group (*H. gigas* and *A. gigantea*) possessed significantly higher levels of TMAO than the shallow-water *P. vannamei* across all the eight tissues (Figure 2a). Different from TMAO, only five tissues (brain, gonad, gut, liver, muscle) exhibited significant differences between the two groups (Figure 2b).

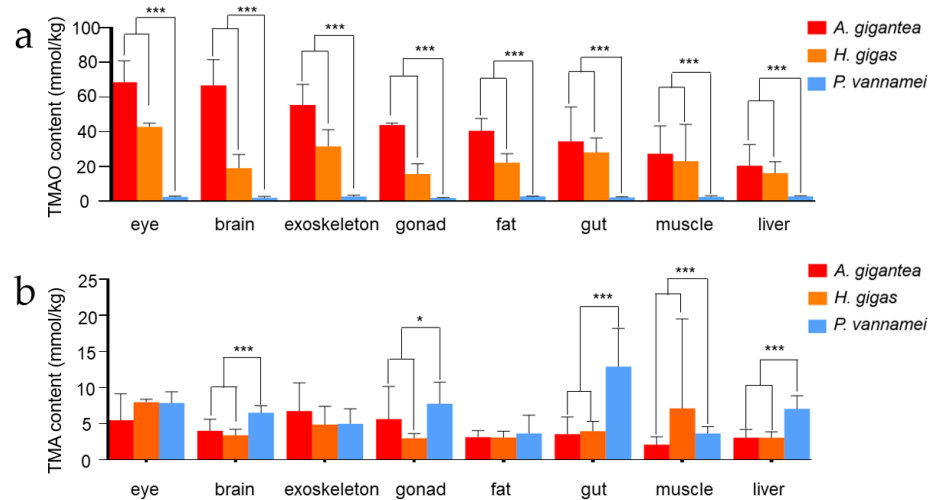


Figure 2. (a,b) TMAO and TMA content in eight tissues (eye, brain, muscle, exoskeleton, gonad, fat, gut, muscle and liver) content in *A. gigantea*, *H. gigas* and *P. vannamei* (unit: mmol/kg wet weight; mean \pm SD). * represents significant difference ($p < 0.05$), and *** represents significant difference ($p < 0.001$).

3.2. Expression Profiling of TMAO and TMA in the Two Hadal Amphipods

In order to compare the tissue expression profiling of TMAO and TMA between the hadal amphipods and the shallow-water species, we drew a heat map regarding all the data derived from Table 1 (TMAO) and Table 2 (TMA). As shown in the heat map (Figure 3), a higher level of TMAO was detected in the external organs (such as the eye and exoskeleton) for both of the two hadal amphipods, which indicated that the TMAO concentration was not evenly distributed, although the same hydrostatic pressure existed in the outer and internal organs (Figure 3a). It also should be noticed that the TMAO content in each tissue of *A. gigantea* was higher than that of *H. gigas*, which might indicate that the TMAO content was not only correlated with the distribution depth.

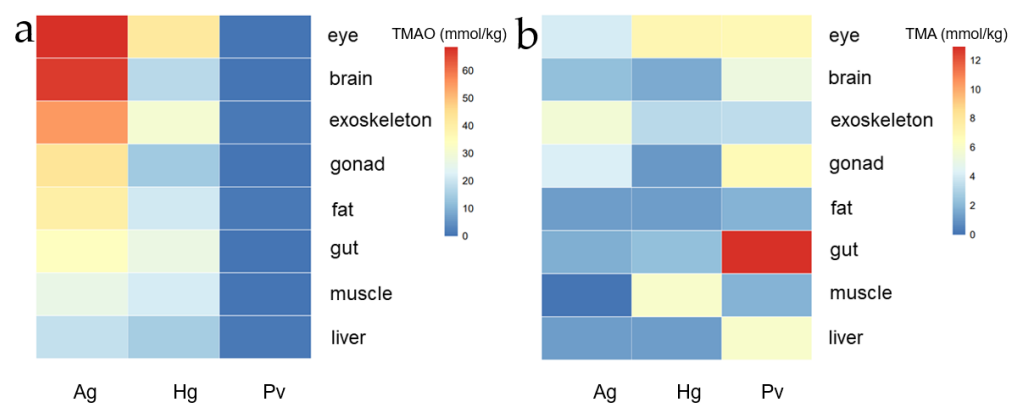


Figure 3. (a,b) TMAO and TMA concrete content in eight tissues (eye, brain, muscle, exoskeleton, gonad, fat, gut, muscle and liver) content in *A. gigantea*, *H. gigas* and *P. vannamei* (unit: mmol/kg wet weight; mean \pm SD).

On the other hand, the TMA showed a different expression profiling among the three species. Generally, a similar level of TMA concentration was detected in *P. vannamei* in most of the detected tissues except for gonad, gut and liver (Figure 3b). The higher-level TMA concentrations detected in *P. vannamei* might indicate less TMA was converted to TMAO when at lower hydrostatic pressures. TMA content reached the highest level in the shallow-water *P. vannamei* gut tissue among all the three species (Figure 3b).

3.3. Correlation Analysis with TMAO and TMA Concentrations

Figure 4 showed a correlation (Pearson method) of TMA and TMAO concentrations of eight tissues in three species. There is an obvious marker that shows that in nine tissues of three species, the order of correlation coefficient between TMAO and TMA corresponding to each tissue is $Hg > Ag > Pv$ (Figure 4a), and a strong positive correlation was found between the concentrations of TMAO and TMA in the two hadal amphipods (Figure 4b,c). It should be noticed that, with the increase in depth, the correlation is stronger ($Hg > Ag$). The strongest correlation in Ag is gonad, and in Hg, the strongest correlation tissue is liver (Figure 4a). However, there was no significant correlation between the tissues in the shallow-water *P. vannamei* (Figure 4d). This suggested to us that there might exist remarkable differences in the TMAO and TMA transformation processes between the hadal amphipods and shallow-water decapods.

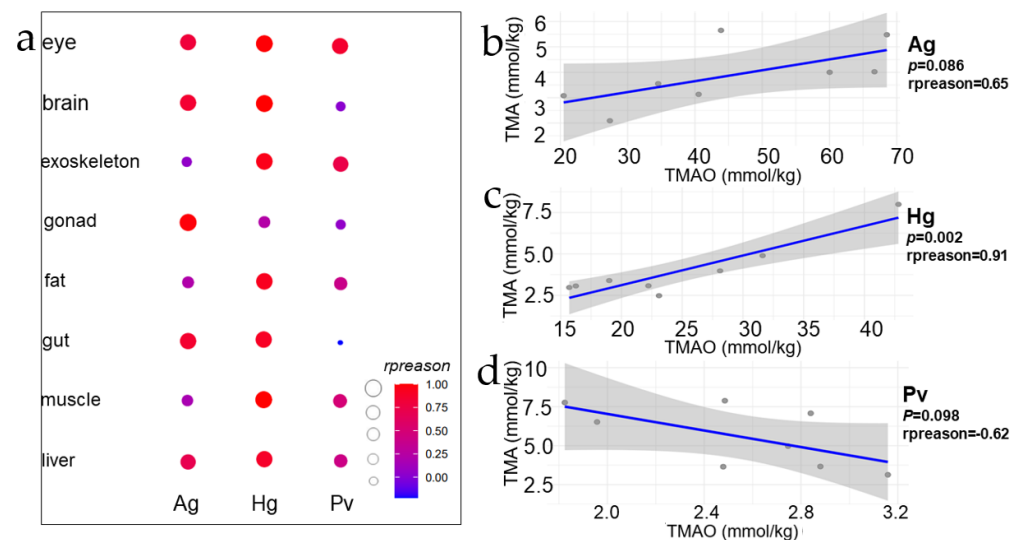


Figure 4. TMAO–TMA correlation comparison and fitting curve. (a) represents the TMAO–TMA correlation scatter plot of each tissue of the two hadal amphipod species, and the size and color of each point represent the magnitude of correlation coefficient. (b–d) represents the fitting curve of the order of *A. gigantea*, *H. gigas* and *P. vannamei*, with Pearson correlation coefficient and *p* value, respectively.

3.4. FMO3 Gene Analysis and Prediction of Three-Dimensional Crystal Structure

FMO3 is the most important TMA oxidase and converts TMA to TMAO [34,37]. In order to conduct the evolutionary analysis regarding FMO3, we based it on the phylogenetic tree constructed by the available published transcriptome data [42,43] (see Supplementary Figure S1). Supplementary Figure S2 shows the phylogenetic tree of FMO3 with the branch lengths in Gammaroidea and *A. gigantea*. As shown in Supplementary Figures S1 and S2, Gammaroidea is the closed clade to *A. gigantea*. Therefore, positive selection analysis regarding FMO3 of *A. gigantea* was performed. By setting the *A. gigantea* as the foreground branch, and other shallow-water Gammaroidea (*Echinogammarus marinus*, *Gammarus fossarum*, *Gammarus chevreuxi* and *Gammarus minus*) as the background species, we conducted the PSG analysis regarding *A. gigantea* FMO3. The FMO3 sequences for the background species are deduced from the SRA database (<https://www.ncbi.nlm.nih.gov/sra>, accessed on 5 February 2022) (*G. fossarum* ERR386132, *G. minus* SRR5576331, SRR5576333, *G. chevreuxi* SRR5109803, SRR5109804, SRR5109805, *E. marinus* SRR8089734, SRR8089735, *A. gigantea* PRJNA739006). We performed positively selected analysis by branch site model. Three positive selected sites (92S, 260A, 286 K) were found in the *A. gigantea* FMO3 gene, although likelihood ratio test (LRT) is not significant for the whole branch.

It should be noticed that some specific protein mutation sites were detected in the hadal amphipod *A. gigantea* (Supplementary Table S1). To our surprise, we found two specific sites in FAD binding motifs (GXGXXG) and FMO identifying motifs (FXGXXXHXXXF/Y) in *A. gigantea* in 9G and 176 V (Figure 5a,b). In *A. gigantea* FMO3, alanine to glycine mutations exist in FAD-binding motifs, and threonine to valine mutations exist in FMO-identifying motifs, while these two mutations do not exist in the four background species (Figure 5b), which might promote the hadal amphipod's FMO3 functions. Moreover, I-TASSER [44] was used to predict the crystal structure of the FMO3 sequence of *A. gigantea* (Figure 5a). The FAD-binding motifs and FAD ligands indicated that this mutation occurred in the conserved FDA-identifying motifs. Therefore, these positive and specific sites of *A. gigantea* FMO3 might help to adapt to the hadal environment.

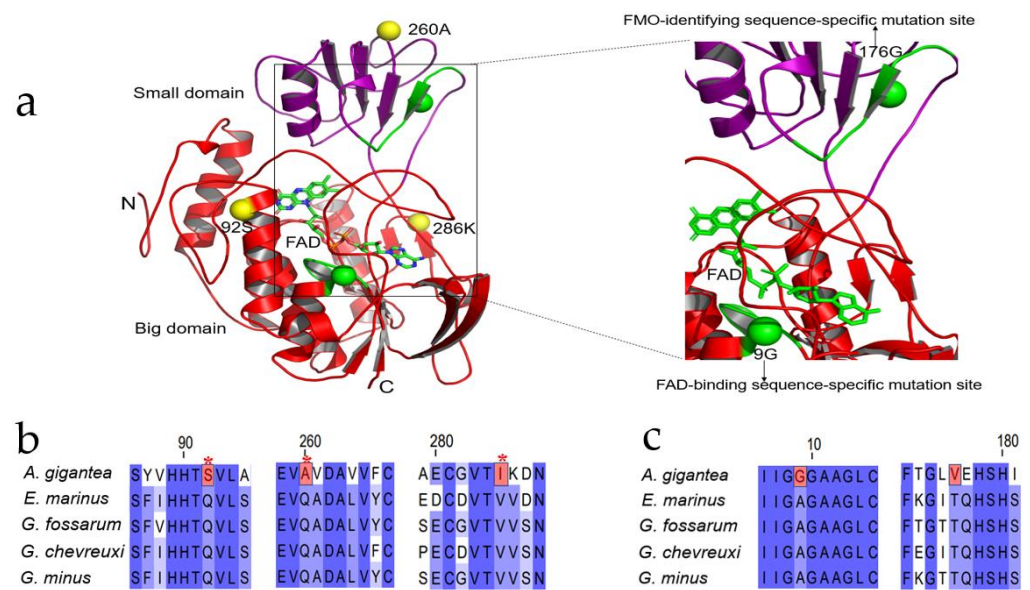


Figure 5. The three-dimensional crystal structure of FMO3 gene of *A. gigantea* and the positively selected site and specific mutation site of the FMO3 gene, (a) represents a three-dimensional view of the FMO3 protein, highlighting the locations of three positive selected sites (yellow spheres) and specific substitution sites on two conserved motifs (green spheres). Conserved motifs and the ligand FAD are also represented in green; (b) represents the location of positively selected sites in *A. gigantea*. Positively selected sites are represented in red, and * represents $p < 0.05$; (c) represents the locations of specific mutation sites that occur on a conserved motif in *A. gigantea* compared with the four amphipods in Gammaroidea, marked in red.

4. Discussion

The hadal zone is the deepest and most mysterious habitat on earth [45]. In hadal trench environments, amphipods appear to be vertically stratified, and species are confined to a relatively narrow depth range within each trench. Meanwhile, the high hydrostatic pressure of the hadal zone is considered to be one of the major obstacles for species to adapt to the hadal environment [46,47]. Different hadal amphipods live at specific depths, and they dominate scavenging communities and are regarded as the primary prey of hadal predators [48]. Accordingly, the study of amphipods is of great importance to the understanding of hadal environment adaptations and amphipods are often used as biological indicators of the hadal environment [49].

Based on these, in this study, we measured the TMAO and TMA concentrations of two hadal amphipods and compared with the values of the shallow-water *Penaeus vannamei*. The overall TMAO content was much higher in the hadal amphipods' tissues (Table 1, Figures 1a, 2a and 3a). Previous studies on hadal fish as well as hadal microbes have proved that HHP will gradually increase with the increase in depth, and the accumulation of TMAO in the body will gradually increase to resist high hydrostatic pressure [23,27].

However, our research shows the TMAO content in each tissue of *A. gigantea* (8824 m) was higher than that of *H. gigas* (10,839 m) (Figure 3a), which might indicate that the TMAO content is not only correlated with the distribution depth, but also related to the particular species. In fact, the two hadal amphipods were sampled from different trenches. It was reported that different TMAO concentrations were detected between the Kermadec Trench and the Mariana Trench at the same depth. However, the TMAO content increases linearly when in the same environment [30]. Since the TMAO is produced in cell and the dead animals will reduce TMAO to TMA [50], it is possible that *A. gigantea* tissues have more intracellular and less extracellular space than tissues of *H. gigas*; therefore, *H. gigas* could have more TMAO inside cells than *A. gigantea*, and it should not be overlooked how long these specimens suffered until they were pulled to the surface. Compared with *A. gigantea* (8824 m), it took a longer time to collect *H. gigas* (10,839 m) samples, which suggested that more TMAO might be converted to TMA in *H. gigas*. The TMA data happened to show that TMA content is higher in *H. gigas* than in *A. gigantea* (Figure 3b).

It should be noticed that a higher level of TMAO was detected in the external organs (such as eye and exoskeleton) for both of the two hadal amphipods (Figure 3a). Previous studies have shown that TMAO can over-stabilize proteins and reduce protein activities and functions in an excessive concentration [51]. However, the normal activities of the hadal species are mainly determined by tissues, internal organs and proteases. There may exist a transport mechanism that transport TMAO in internal organs to external organs to keep the TMAO in a balanced concentration.

TMA has been reported to be produced by gut microbes in hadal fishes [52]. Different depths and the gut microbe's diversity in different amphipods are different [53], and the available nitrogen sources may decrease as the depth increases. TMA production is also affected by the interaction between intestinal microorganisms and hadal amphipod species [3]. As shown in Figure 3b, the tissues with the highest TMA content are found in the intestine of *P. vannamei*. It was well known that the liver is considered to be the main site of TMAO production in mammals [54]. The highest TMA content located in *P. vannamei*'s gut revealed that the nitrogen source is sufficient in *P. vannamei* and TMA in crustaceans might also be produced by gut microbes. The *P. vannamei* samples were captured in Qingdao, but during the transporting process to Shanghai, unfortunately it was not possible to keep it constantly at -80°C . In transit, the TMA in *P. vannamei* probably started to convert TMA to TMAO in the gut by bacteria [55].

The muscle TMAO content is nearly 400 mmol/kg in snailfish when the depth is nearly 8000 m and is nearly 200 mmol/kg in deep-sea decapods when the depth is nearly 2000 m [29]. However, our data showed the highest TMAO content in eight tissues is 68 mmol/kg in hadal amphipods and it is obviously lower than those two species. At the same time, the TMAO content has been reported to exist in the cell [50]. The tissue samples used in our study may contain non-cell parts and the cell structure may also have been broken during the tissue dissection process, which could be the possible reason for the lower TMAO concentrations detected in our study.

Not only TMAO, but also TMA, plays an important role in marine ecosystems as a major precursor of the greenhouse gas methane in coastal sediments [56]. It has also been demonstrated that microorganisms in the deep ocean absorb TMA from the environment and convert it to TMAO to offset HHP [27]. Our study shows a strong positive correlation between the two hadal amphipod TMAO–TMA species in deeper waters, but this correlation was not confirmed in the shallow-water *P. vannamei*.

It was well known that the conversion of TMA to TMAO is accomplished through the FMO3 gene. The FMO gene has also been shown to prolong life and maintain structural stability [57]. Therefore, the study of amphipods may reveal many phenomena of the hadal environment and adaptive evolution of species. In this study, we used the hadal amphipod *A. gigantea*'s FMO3 gene to analyze the selected pressure of the hadal amphipod species and found that FMO3 sequences generally did not have the positive selection in the entire nucleic acid evolutionary branches of hadal species. Structural adaptations of proteins to

hadal conditions may include patterns of amino acid substitution and changes in protein structure that counteract the effects of stress on protein function, and even evolutionary patterns of some proteins that respond to hydrostatic pressure [7,58]. Indeed, Mariana Trench snailfish (MHS) also exhibit a positive selected site in FMO. It not even have a closed skull as the bone Gla protein (*bglap*) gene has a frameshift mutation that may cause the premature termination of cartilage calcification in the MHS [34].

Therefore, proteins at some sites are positively selected to adapt to high hydrostatic pressure to maintain structural stability. The FMO3 was observed in two FAD-specific binding motifs in the *A. gigantea*, and two FMO3-conserved motifs are mutated at specific sites. Therefore, the substitution of such a conserved site suggests that this mutation may be functionally beneficial to the protein functional adaptation of hadal species to hadal environments. FMO3 is an evolutionarily conserved and highly abundant redox enzyme system. The crystal structure of the FMO3 protein of *A. gigantea* was predicted by the threading method as shown in Supplementary Figure S3. Factually, the genomic gene family expansion, amino acid substitution and copy number increase are also important regulatory mechanisms. Like HSPs in the hadal amphipod and fish, the HSP in *H. gigas* can have more copies and some special site mutations. Other species help adapt HHP; the λ_{\max} of rhodopsin 1 in YHS (Yap hadal snailfish) and MHS rhodopsin are lower than the levels found in shallow-water teleosts and may help them adapt to dark environments in the hadal zone [34,59,60]. All in all, the concrete intrinsic adaptation is complicated. Further studies of specific structure and function will clarify the specific effects of this unique mutation on the FMO3 protein. The concrete mechanism about how the hadal species adapt to the hadal environment is still to be researched.

5. Conclusions

In this study, we measured the TMAO and TMA content in eight tissues of two hadal amphipod species, and a shallow water decapod, *P. vannamei*. We found that the TMAO content in hadal amphipod species is much higher than that in shallow species, and also found that in amphipods, there may be a strong positive TMAO–TMA correlation among amphipods in hadal habitats. We also found specific loci changes on two conserved motifs in the FMO3 gene of the hadal amphipod. This study provides insights into the molecular adaptation mechanisms of hadal organisms.

Supplementary Materials: The following supporting information can be downloaded at: <https://www.mdpi.com/article/10.3390/jmse10040454/s1>. Figure S1: The phylogenetic position of the *Hirondellea gigas* and *Alicella gigantea* based on maximum likelihood (ML) estimation of FMO3 gene of selected crustacean species. Figure S2: Phylogenetic tree of FMO3 with the branch lengths between Gammaroidea and *A. gigantea*. Figure S3: The prediction of three-dimensional crystal structure of FMO3 protein of *A. gigantea*; Table S1: The positive selected sites and specific substitution sites on two conserved motifs.

Author Contributions: Validation, Q.L., S.J. and W.L.; formal analysis, Q.L.; data curation, Q.L., S.J. and W.L.; sampling, B.P.; writing—original draft preparation, Q.L. and S.J.; writing—review and editing, Q.X.; visualization, Q.L.; supervision, Q.X.; project administration, Q.X.; funding acquisition, Q.X. All authors have read and agreed to the published version of the manuscript.

Funding: This research was funded in part by the Funding Project of the National Key Research and Development Program of China (2018YFC0310600), the National Key Research and Development Program of China (2018YFD0900601), the National Natural Science Foundation of China (Grant No. 31772826), and the major scientific innovation project from Shanghai Committee of Education (2017-01-07-00-10-E00060).

Institutional Review Board Statement: Not applicable.

Informed Consent Statement: Not applicable.

Data Availability Statement: Not applicable.

Acknowledgments: We would like to thank Shanghai Rainbowfish Ocean Technology Co., Ltd., for sample collection. We also thank Weicheng Cui's and Jiasong Fang's research group members and other people for sample collection.

Conflicts of Interest: The authors declare no conflict of interest.

References

1. Cressey, D. The Hadal Zone: Life in the Deepest Oceans. *Nature* **2015**, *523*, SB1.
2. Weston, J.N.J.; Espinosa-Leal, L.; Wainwright, J.A.; Stewart, E.C.D.; Gonzalez, C.E.; Linley, T.D.; Reid, W.D.K.; Hidalgo, P.; Oliva, M.E.; Ulloa, O.; et al. *Eurythenes atacamensis* sp. nov. (Crustacea: Amphipoda) exhibits ontogenetic vertical stratification across abyssal and hadal depths in the Atacama Trench, eastern South Pacific Ocean. *Mar. Biodivers.* **2021**, *51*, 51. [CrossRef] [PubMed]
3. Chan, J.L.; Geng, D.Q.; Pan, B.B.; Zhang, Q.M.; Xu, Q.H. Metagenomic Insights Into the Structure and Function of Intestinal Microbiota of the Hadal Amphipods. *Front. Microbiol.* **2021**, *12*. Available online: <https://www.frontiersin.org/articles/10.3389/fmicb.2021.668989/full> (accessed on 5 February 2022). [CrossRef]
4. Zhang, W.P.; Tian, R.M.; Sun, J.; Bougouffa, S.; Ding, W.; Cai, L.; Lan, Y.; Tong, H.Y.; Li, Y.X.; Jamieson, A.J.; et al. Genome Reduction in Psychromonas Species within the Gut of an Amphipod from the Ocean's Deepest Point. *Msystems* **2018**, *3*, e00009-18. [CrossRef] [PubMed]
5. Bartlett, D.H. Microbial life at high pressures. *Sci. Prog.* **1992**, *76*, 479–496. [PubMed]
6. Jamieson, A.J.; Fujii, T.; Mayor, D.J.; Solan, M.; Priede, I.G. Hadal trenches: The ecology of the deepest places on Earth. *Trends Ecol. Evol.* **2010**, *25*, 190–197. [CrossRef] [PubMed]
7. Somero, G.N. Adaptations to high hydrostatic pressure. *Annu. Rev. Physiol.* **1992**, *54*, 557–577. [CrossRef] [PubMed]
8. Macdonald, A.G. Hydrostatic pressure as an environmental factor in life processes. *Comp. Biochem. Phys. A* **1997**, *116*, 291–297. [CrossRef]
9. Thurston, M.H. Scavenging abyssal amphipods from the North-East Atlantic ocean. *Mar. Biol.* **1979**, *51*, 55–68. [CrossRef]
10. Blankenship, L.E.; Yyanos, A.A.; Cadien, D.B.; Levin, L.A. Vertical zonation patterns of scavenging amphipods from the Hadal zone of the Tonga and Kermadec Trenches. *Deep Sea Res. Part I Oceanogr. Res. Pap.* **2006**, *53*, 48–61. [CrossRef]
11. Beliaev, G.M.; Vinogradov, M.Y. Deep-sea ocean trenches and their fauna. *Scripps Inst. Oceanogr.* **1989**. Available online: <https://escholarship.org/uc/item/46n6148x> (accessed on 5 February 2022).
12. Jamieson, A.J.; Lacey, N.C.; Lorz, A.N.; Rowden, A.A.; Piertney, S.B. The supergiant amphipod *Alicella gigantea* (Crustacea: Alicellidae) from hadal depths in the Kermadec Trench, SW Pacific Ocean. *Deep Sea Res. Part II Top. Stud. Oceanogr.* **2013**, *92*, 107–113. [CrossRef]
13. Zhu, L.Y.; Geng, D.Q.; Pan, B.B.; Li, W.H.; Jiang, S.W.; Xu, Q.H. Trace Elemental Analysis of the Exoskeleton, Leg Muscle, and Gut of Three Hadal Amphipods. *Biol. Trace Elem. Res.* **2021**, *200*, 1395–1407. [CrossRef] [PubMed]
14. Kobayashi, H.; Hatada, Y.; Tsubouchi, T.; Nagahama, T.; Takami, H. The Hadal Amphipod *Hirondellea gigas* Possessing a Unique Cellulase for Digesting Wooden Debris Buried in the Deepest Seafloor. *PLoS ONE* **2012**, *7*, e42727. [CrossRef] [PubMed]
15. Silva, J.L.; Vieira, T.C.R.G.; Gomes, M.P.B.; Bom, P.A.; Lima, L.M.T.R.; Freitas, M.S.; Ishimaru, D.; Cordeiro, Y.; Foguel, D. Ligand Binding and Hydration in Protein Misfolding: Insights from Studies of Prion and p53 Tumor Suppressor Proteins. *Acc. Chem. Res.* **2010**, *43*, 271–279. [CrossRef] [PubMed]
16. Lan, Y.; Sun, J.; Xu, T.; Chen, C.; Tian, R.M.; Qiu, J.W.; Qian, P.Y. De novo transcriptome assembly and positive selection analysis of an individual deep-sea fish. *BMC Genom.* **2018**, *19*, 1–9. [CrossRef]
17. Brooks, N.J. Pressure effects on lipids and bio-membrane assemblies. *IUCrJ* **2014**, *1*, 470–477. [CrossRef]
18. Somero, G.N. Protein adaptations to temperature and pressure: Complementary roles of adaptive changes in amino acid sequence and internal milieu. *Comp. Biochem. Phys. B* **2003**, *136*, 577–591. [CrossRef]
19. Morris, J.P.; Thatje, S.; Hauton, C. The use of stress-70 proteins in physiology: A re-appraisal. *Mol. Ecol.* **2013**, *22*, 1494–1502. [CrossRef]
20. Genest, O.; Wickner, S.; Doyle, S.M. Hsp90 and Hsp70 chaperones: Collaborators in protein remodeling. *J. Biol. Chem.* **2019**, *294*, 2109–2120. [CrossRef]
21. Yancey, P.H. Organic osmolytes as compatible, metabolic and counteracting cytoprotectants in high osmolarity and other stresses. *J. Exp. Biol.* **2005**, *208*, 2819–2830. [CrossRef]
22. Wang, Z.; Klipfell, E.; Bennett, B.J.; Koeth, R.; Levison, B.S.; Dugar, B.; Feldstein, A.E.; Britt, E.B.; Fu, X.; Chung, Y.M.; et al. Gut flora metabolism of phosphatidylcholine promotes cardiovascular disease. *Nature* **2011**, *472*, 57–63. [CrossRef] [PubMed]
23. Canyelles, M.; Tondo, M.; Cedo, L.; Farras, M.; Escola-Gil, J.C.; Blanco-Vaca, F. Trimethylamine N-Oxide: A Link among Diet, Gut Microbiota, Gene Regulation of Liver and Intestine Cholesterol Homeostasis and HDL Function. *Int. J. Mol. Sci.* **2018**, *19*, 3228. [CrossRef] [PubMed]
24. Jamieson, D.A. Marine fish may be biochemically constrained from inhabiting deepest ocean depths. *Proc. Natl. Acad. Sci. USA* **2014**, *111*, 4461–4465.
25. Yancey, P.H. Cellular responses in marine animals to hydrostatic pressure. *J. Exp. Zool. Part A* **2020**, *333*, 398–420. [CrossRef] [PubMed]

26. Bolen, D.W.; Baskakov, I.V. The osmophobic effect: Natural selection of a thermodynamic force in protein folding. *J. Mol. Biol.* **2001**, *310*, 955–963. [CrossRef]
27. Qin, Q.L.; Wang, Z.B.; Su, H.N.; Chen, X.L.; Miao, J.; Wang, X.J.; Li, C.Y.; Zhang, X.Y.; Li, P.Y.; Wang, M.; et al. Oxidation of trimethylamine to trimethylamine N-oxide facilitates high hydrostatic pressure tolerance in a generalist bacterial lineage. *Sci. Adv.* **2021**, *7*, eabf9941. [CrossRef]
28. Yancey, P.H.; Speers-Roesch, B.; Atchinson, S.; Reist, J.D.; Majewski, A.R.; Treberg, J.R. Osmolyte Adjustments as a Pressure Adaptation in Deep-Sea Chondrichthyan Fishes: An Intraspecific Test in Arctic Skates (*Amblyraja hyperborea*) along a Depth Gradient. *Physiol. Biochem. Zool.* **2018**, *91*, 788–796. [CrossRef]
29. Kelly, R.H.; Yancey, P.H. High Contents of Trimethylamine Oxide Correlating with Depth in Deep-Sea Teleost Fishes, Skates, and Decapod Crustaceans. *Biol. Bull.* **1999**, *196*, 1825. [CrossRef]
30. Downing, A.B.; Wallace, G.T.; Yancey, P.H. Organic osmolytes of amphipods from littoral to hadal zones: Increases with depth in trimethylamine N-oxide, scyllo-inositol and other potential pressure counteractants. *Deep Sea Res. Part I Oceanogr. Res. Pap.* **2018**, *138*, 1–10. [CrossRef]
31. Linley, T.D.; Gerringer, M.E.; Yancey, P.H.; Drazen, J.C.; Weinstock, C.L.; Jamieson, A.J. Fishes of the hadal zone including new species, in situ observations and depth records of Liparidae. *Deep-Sea Res. Part I* **2016**, *114*, 99–110. [CrossRef]
32. Swan, J.A.; Jamieson, A.J.; Linley, T.D.; Yancey, P.H. Worldwide distribution and depth limits of decapod crustaceans (Penaeoidea, Oplophoroidea) across the abyssal-hadal transition zone of eleven subduction trenches and five additional deep-sea features. *J. Crustacean Biol.* **2021**, *41*, ruaa102. [CrossRef]
33. Winnikoff, J.R.; Wilson, T.M.; Thuesen, E.V.; Haddock, S.H.D. Enzymes feel the squeeze: Biochemical adaptation to pressure in the deep sea. *Biochemist* **2017**, *39*, 26–29. [CrossRef]
34. Wang, K.; Shen, Y.; Yang, Y.; Gan, X.; Liu, G.; Hu, K.; Li, Y.; Gao, Z.; Zhu, L.; Yan, G. Morphology and genome of a snailfish from the Mariana Trench provide insights into deep-sea adaptation. *Nat. Ecol. Evol.* **2019**, *3*, 823–833. [CrossRef] [PubMed]
35. Van Berkel, W.J.H.; Kamerbeek, N.M.; Fraaije, M.W. Flavoprotein monooxygenases, a diverse class of oxidative biocatalysts. *J. Biotechnol.* **2006**, *124*, 670–689. [CrossRef]
36. Eswaramoorthy, S.; Bonanno, J.B.; Burley, S.K.; Swaminathan, S. Mechanism of action of a flavin-containing monooxygenase. *Proc. Natl. Acad. Sci. USA* **2006**, *103*, 9832–9837. [CrossRef]
37. Huang, S.; Howington, M.B.; Dobry, C.J.; Evans, C.R.; Leiser, S.F. Flavin-Containing Monooxygenases Are Conserved Regulators of Stress Resistance and Metabolism. *Front. Cell Dev. Biol.* **2021**, *9*, 630188. [CrossRef]
38. Beaty, N.B.; Ballou, D.P. The oxidative half-reaction of liver microsomal FAD-containing monooxygenase. *J. Biol. Chem.* **1981**, *256*, 4619–4625. [CrossRef]
39. Wu, Q.; Zhao, Y.; Zhang, X.; Yang, X. A faster and simpler UPLC-MS/MS method for the simultaneous determination of trimethylamine N-oxide, trimethylamine and dimethylamine in different types of biological samples. *Food Funct.* **2019**, *10*, 6484–6491. [CrossRef]
40. Gao, F.; Chen, C.; Arab, D.A.; Du, Z.; He, Y.; Ho, S.Y.W. EasyCodeML: A visual tool for analysis of selection using CodeML. *Ecol. Evol.* **2019**, *9*, 3891–3898. [CrossRef]
41. Zerbst-Boroffka, I.; Kamaltynow, R.M.; Harjes, S.; Kinne-Saffran, E.; Gross, J. TMAO and other organic osmolytes in the muscles of amphipods (Crustacea) from shallow and deep water of Lake Baikal. *Comp. Biochem. Physiol. Part A Mol. Integr. Physiol.* **2005**, *142*, 58–64. [CrossRef]
42. Li, W.H.; Wang, F.X.; Jiang, S.W.; Pan, B.B.; Chan, J.L.; Xu, Q.H. The Adaptive Evolution and Gigantism Mechanisms of the Hadal “Supergiant” Amphipod *Alicella gigantea*. *Front. Mar. Sci.* **2021**, *8*. Available online: <https://www.frontiersin.org/articles/10.3389/fmars.2021.743663/full> (accessed on 5 February 2022). [CrossRef]
43. Copilas-Ciocianu, D.; Borko, S.; Fiser, C. The late blooming amphipods: Global change promoted post-Jurassic ecological radiation despite Palaeozoic origin. *Mol. Phylogenet. Evol.* **2020**, *143*, 106664. [CrossRef] [PubMed]
44. Zheng, W.; Zhang, C.; Li, Y.; Pearce, R.; Zhang, Y. Folding non-homologous proteins by coupling deep-learning contact maps with I-TASSER assembly simulations. *Cell Rep. Methods* **2021**, *1*, 100014. [CrossRef]
45. Piccard, J. Man’s deepest dive. *Natl. Geogr.* **1960**, *118*, 224–239.
46. Brown, A.; Thatje, S. Explaining bathymetric diversity patterns in marine benthic invertebrates and demersal fishes: Physiological contributions to adaptation of life at depth. *Biol. Rev.* **2013**, *89*, 406–426. [CrossRef] [PubMed]
47. Smith, K.E.; Brown, A.; Thatje, S. The metabolic cost of developing under hydrostatic pressure: Experimental evidence supports macroecological pattern. *Mar. Ecol. Prog. Ser.* **2015**, *524*, 71–82. [CrossRef]
48. Jamieson, A.J.; Fujii, T.; Solan, M.; Matsumoto, A.K.; Bagley, P.M.; Priede, I.G. First findings of decapod crustacea in the hadal zone. *Deep Sea Res. Part I Oceanogr. Res. Pap.* **2009**, *56*, 641–647. [CrossRef]
49. Hupalo, K.; Teixeira, M.A.L.; Rewicz, T.; Sezgin, M.; Iannilli, V.; Karaman, G.S.; Grabowski, M.; Costa, F.O. Persistence of phylogeographic footprints helps to understand cryptic diversity detected in two marine amphipods widespread in the Mediterranean basin. *Mol. Phylogenet. Evol.* **2019**, *132*, 53–66. [CrossRef]
50. Gillett, M.B.; Suko, J.R.; Santoso, F.O.; Yancey, P.H. Elevated levels of trimethylamine oxide in muscles of deep-sea gadiform teleosts: A high-pressure adaptation? *J. Exp. Zool.* **1997**, *279*, 386–391. [CrossRef]
51. Yancey, P.H.; Clark, M.E.; Hand, S.C.; Bowlus, R.D.; Somero, G.N. Living with water stress: Evolution of osmolyte systems. *Science* **1982**, *217*, 1214–1222. [CrossRef]

-
52. Subramaniam, S.; Fletcher, C. Trimethylamine N-oxide: Breathe new life. *Br. J. Pharmacol.* **2018**, *175*, 1344–1353. [[CrossRef](#)] [[PubMed](#)]
 53. Chan, J.; Geng, D.; Pan, B.; Zhang, Q.; Xu, Q. Gut Microbial Divergence Between Three Hadal Amphipod Species from the Isolated Hadal Trenches. *Microb. Ecol.* **2021**, 1–11. [[CrossRef](#)]
 54. Janeiro, M.H.; Ramirez, M.J.; Milagro, F.I.; Martinez, J.A.; Solas, M. Implication of Trimethylamine N-Oxide (TMAO) in Disease: Potential Biomarker or New Therapeutic Target. *Nutrients* **2018**, *10*, 1398. [[CrossRef](#)] [[PubMed](#)]
 55. Zhang, W.Q.; Wang, Y.J.; Zhang, A.; Ding, Y.J.; Zhang, X.N.; Jia, Q.J.; Zhu, Y.P.; Li, Y.Y.; Lv, S.C.; Zhang, J.P. TMA/TMAO in Hypertension: Novel Horizons and Potential Therapies. *J. Cardiovasc. Transl. Res.* **2021**, *14*, 1117–1124. [[CrossRef](#)]
 56. King, G.M. Metabolism of trimethylamine, choline, and glycine betaine by sulfate-reducing and methanogenic bacteria in marine sediments. *Appl. Environ. Microbiol.* **1984**, *48*, 719–725. [[CrossRef](#)]
 57. Leiser, S.F.; Miller, H.; Rossner, R.; Fletcher, M.; Leonard, A.; Primitivo, M.; Rintala, N.; Ramos, F.J.; Miller, D.L.; Kaeberlein, M. Cell nonautonomous activation of flavin-containing monooxygenase promotes longevity and health span. *Science* **2015**, *350*, 1375–1378. [[CrossRef](#)]
 58. Yafremava, L.S.; Di Giulio, M.; Caetano-Anolles, G. Comparative analysis of barophily-related amino acid content in protein domains of *Pyrococcus abyssi* and *Pyrococcus furiosus*. *Archaea* **2013**, *2013*, 680436. [[CrossRef](#)]
 59. Ritchie, H.; Jamieson, A.J.; Piertney, S.B. Heat-shock protein adaptation in abyssal and hadal amphipods. *Deep Sea Res. Part II Top. Stud. Oceanogr.* **2018**, *155*, 61–69. [[CrossRef](#)]
 60. Mu, Y.; Bian, C.; Liu, R.; Wang, Y.; Shao, G.; Li, J.; Qiu, Y.; He, T.; Li, W.; Ao, J.; et al. Whole genome sequencing of a snailfish from the Yap Trench (~7000 m) clarifies the molecular mechanisms underlying adaptation to the deep sea. *PLoS Genet.* **2021**, *17*, e1009530. [[CrossRef](#)] [[PubMed](#)]